

Water quality monitoring with Sentinel-2 and Landsat-8 satellites during the 2021 volcanic eruption in La Palma (Canary Islands)

Isabel Caballero ^{*}, Alejandro Román, Antonio Tovar-Sánchez, Gabriel Navarro

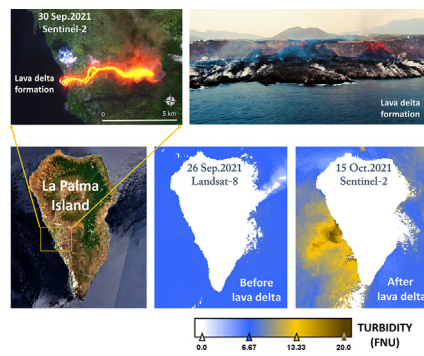
Instituto de Ciencias Marinas de Andalucía (ICMAN), Consejo Superior de Investigaciones Científicas (CSIC), Avenida República Saharaui, 11519 Puerto Real, Spain



HIGHLIGHTS

- Landsat-8 and Sentinel-2 satellites are jointly used to examine the marine impact of a volcanic eruption.
- A consistent pre-processing methodology (atmospheric and sunglint corrections) is implemented.
- Short- and medium-term evolution of the new lava delta and subsequent impact on the seawater was addressed.
- Near-real time mapping of turbidity and chlorophyll-a concentration is accomplished in La Palma Island.
- Multi-sensor products may contribute to enhanced monitoring of water quality during hazards.

GRAPHICAL ABSTRACT



ARTICLE INFO

Article history:

Received 4 December 2021

Received in revised form 17 January 2022

Accepted 22 January 2022

Available online 29 January 2022

Editor: Josá Virgálio Cruz

Keywords:

Remote sensing

Copernicus programme

Hazards

Volcanic eruption

Water quality mapping

Lava delta

ABSTRACT

In this study, seawater quality was monitored with high-resolution satellite imagery during the 2021 volcanic eruption (September–December) on La Palma Island (Spain), the longest recorded in the history of the island, and the most destructive in the last century in Europe. The Sentinel-2A/B twin satellites and Landsat-8 satellite were jointly used as an optical constellation, which allowed us to successfully characterize the short- and medium-term evolution of the new lava delta and subsequent impact on the seawater. Robust atmospheric and sunglint correction approaches were applied to thoroughly quantify the environmental changes caused on the adjacent coastal waters. The cloud and volcanic ash coverage remained very high over the coast during the event, so restricted information with 14 images (45% of the total scenes) was retrieved from the multi-sensor approach. Nevertheless, the availability of pre-, syn-, and post-eruption satellite products allowed us to map and detect the main water quality variations in the marine environment. On the one hand, during the eruption, a change in the properties of the water quality was observed, with a markedly increased turbidity on the western side of the island near the new lava delta due to the deposition of volcanic ash and material. On the other hand, chlorophyll-a concentration did not significantly increase, algal blooms were not observed, and oligotrophic conditions were not swiftly altered towards eutrophic conditions. This information offered an excellent opportunity to characterize the emplacement of the new lava delta and its impact on the marine environment in La Palma. The present multi-sensor strategy is an excellent opportunity to highlight the potential of remote sensing technology as a relevant and powerful tool for future hazard monitoring and assessment during catastrophes and for a better interpretation of their impact on the marine environment.

1. Introduction

^{*} Corresponding author.

E-mail address: isabel.caballero@icman.csic.es (I. Caballero).

Earth processes, extreme weather events, and natural hazards are better understood by utilizing freely available remote sensing observations thanks

to an increase in technological advances and data availability, which can systematically improve science and environmental-monitoring products (Wulder and Coops, 2014; Gray et al., 2020; Rajendran et al., 2021). Satellite technology has become more prominent in the past decade, with constellations, such as the Sentinel-2 from the European Commission's Copernicus programme, that are capable of synoptically observing the state of coastal and inland environments with significantly improved spatio-temporal coverage (Caballero et al., 2019; Bacques et al., 2020; Caballero et al., 2020; Tapete and Cigna, 2020; Caballero and Navarro, 2021; McKee et al., 2021; Normandeau et al., 2021). In particular, high-resolution satellite-based information plays a key role in monitoring the impact of volcanoes located in remote areas with limited in situ monitoring networks (Fraile-Nuez et al., 2012; Coca et al., 2014; Eugenio et al., 2014; Xu and Jónsson, 2014; Plank et al., 2019, 2020; Corradino et al., 2021; Martin et al., 2021).

On 19 September 2021, an eruption began from a new volcano on the Cumbre Vieja ridge, comprising the southern half of La Palma, in the Spanish archipelago of the Canary Islands (Fig. 1). Lava flowed down the

mountain after the crack opened in the volcano, emitting large amounts of volcanic material and ash into the air. The lava destroyed everything in its path before reaching the ocean ten days later, being the most damaging volcanic eruption on La Palma since records began (IGN, 2021). The lava flow in contact with the marine environment rapidly solidified, creating a new lava delta, locally known as "fajana" (Fig. 2), and forming a new peninsula (Bosman et al., 2014; Di Traglia et al., 2018; Zhao et al., 2020). Authorities set up an exclusion zone around the new delta, including the water mass with a 500-meter security perimeter that vessels could not access. Fig. 3 indicates the formation of this fan-shaped mound with a lobate morphology in the western section of La Palma as a result of the volcanic material accumulating on the ocean floor. The Sentinel-2 images before and after the formation of the new strip, on 15 and 30 September 2021, respectively, indicate the change in the coastline (Fig. 3). The newly constructed lava delta continued to grow as hot lava flows entered the sea, extending the coastline outwards: as of 30 September 2021, this was 28 ha in size (Fig. 1d), 34 ha by 10 October 2021 (Fig. 1e), and 35 ha by 15 October 2021 (Fig. 1f). On 25 December 2021, the local government

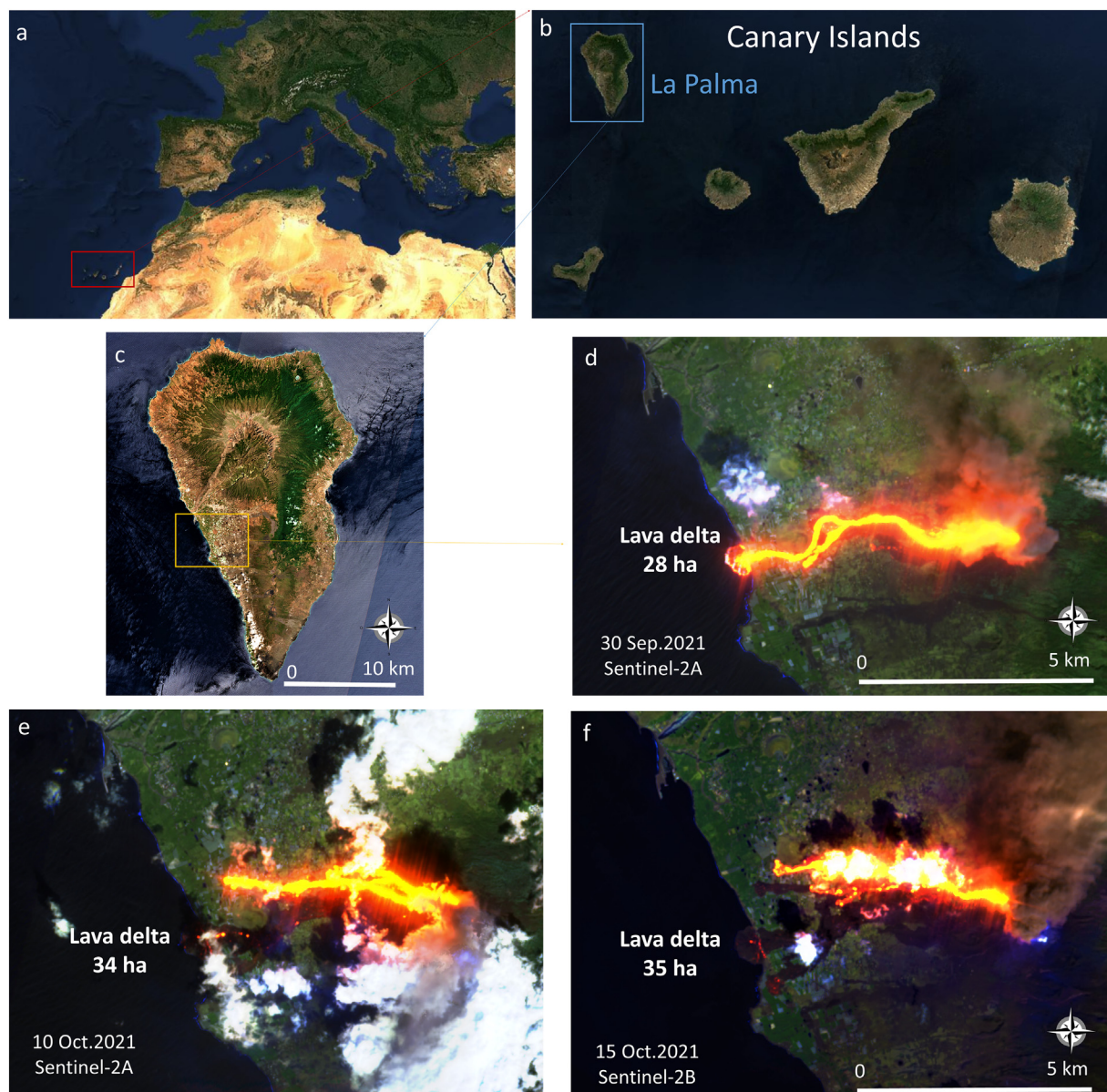


Fig. 1. a) Location of the study area, b) map of the Canary Islands, c) Sentinel-2 pre-eruption image of La Palma Island on 26 August 2021, d) Sentinel-2A post-eruption scene on 30 September 2021 after the formation of the lava delta with an area of 28 ha, e) Sentinel-2A post-eruption scene on 10 October 2021 (lava delta extension of 34 ha), and f) Sentinel-2B post-eruption scene on 15 October 2021 (lava delta extension of 35 ha).

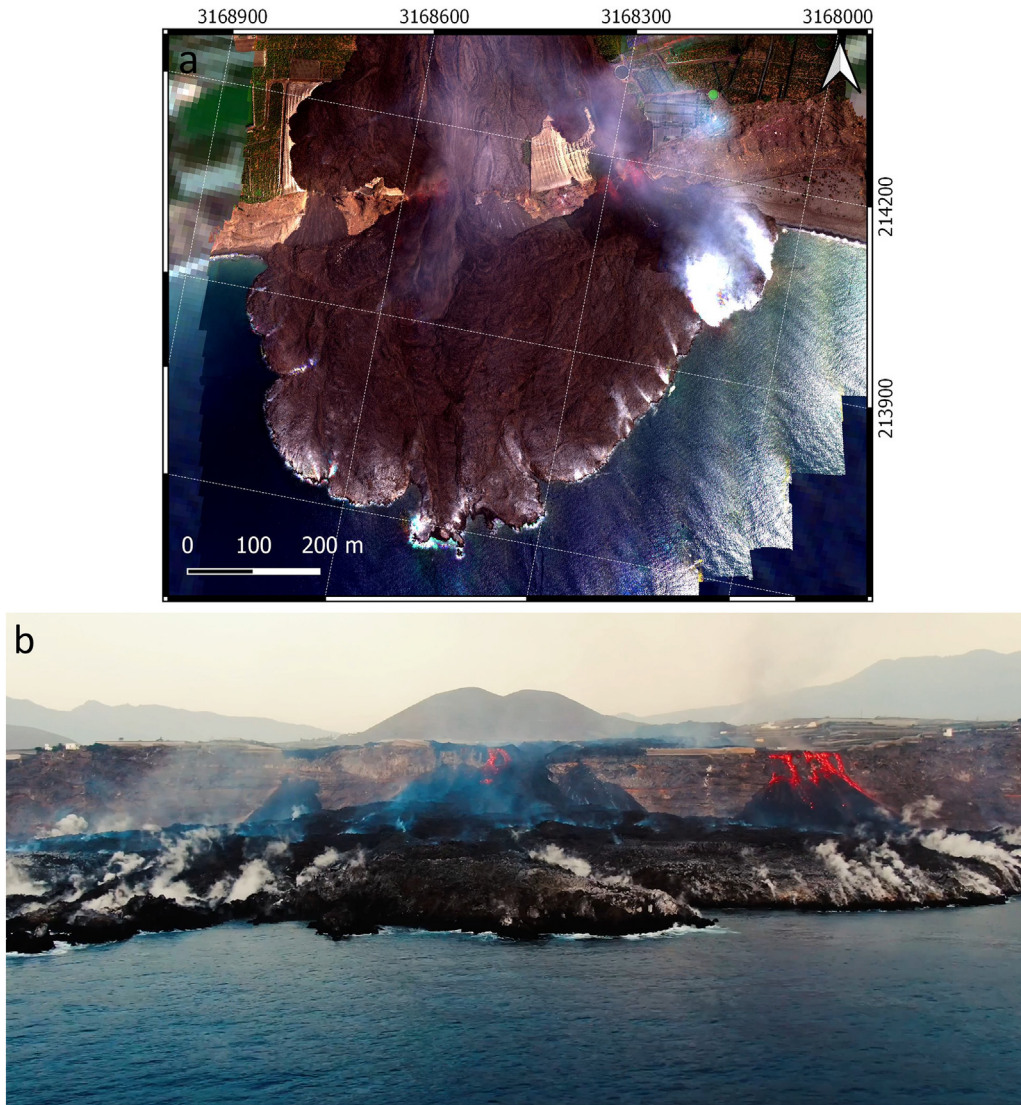


Fig. 2. a) RGB (Red-Green-Blue) composited scene acquired on 2 October 2021 from the MicaSense RedEdge-MX dual multispectral camera onboard the unmanned aerial vehicle (UAV). The UAV allowed very-high resolution (centimeters) monitoring of the new lava delta on the western coast of La Palma Island; b) Photo of the lava-fed delta on the western coast of La Palma collected with an UAV on 2 October 2021. The evolution of the lava flow fields and the main subaerial lava lobes are evident.

officially declared the eruption to be over after three months. The 2021 volcanic eruption in La Palma was the longest eruption recorded in the history of the island, and the most destructive in the last century in Europe (Instituto Geográfico Nacional, 2021).

Thousands of people were evacuated and hundreds of properties were destroyed after the volcanic eruption. The Spanish Government declared La Palma as a disaster zone and prepared a reconstruction plan, a set of immediate measures, and financial support for the people affected. The Copernicus Emergency Management Service (CEMS) Rapid Mapping was activated (EMSR546), following the request of the Spanish General Directorate for Civil Protection and Emergencies (CENEM), to support the emergency response during the volcanic eruption (<https://emergency.copernicus.eu/mapping/list-of-components/EMSR546/>). Both radar and optical satellite data were used for the analysis, depending on availability of usable imagery. As the eruption was ongoing and the situation in La Palma was evolving, in particular with new lava flows as a result of the partial collapse of the main volcanic cone (Instituto Geográfico Nacional, 2021), the Rapid Mapping provided updated information on the eruption detailing the changes in the extent of the ash deposits and lava flow, as well as destroyed roads, buildings, and other infrastructure. Satellite-supported research is compelling and essential for our well-being, as demonstrated during this emergency.

However, the marine environmental impacts of volcanic eruptions on islands, such as La Palma, typically receive significantly less attention than the socio-economic, atmospheric, or land impacts. The volcanic ashes and the formation of the lava delta can alter the biochemical conditions of the surrounding waters, thus severely affecting the marine ecosystem (Lebrato et al., 2019) and fisheries on which an economic sector of the island depends. Coastal waters are frequently characterized by high turbidity and concentrations of suspended inorganic or organic material derived from the activity of volcanoes and lava-delta formation. Peaked turbidity levels can affect many benthic and water column processes such as productivity of phytoplankton or submerged aquatic vegetation, pollutants transport, or nutrient dynamics, yielding a detrimental impact on the ecosystem and increasing the environmental instability (Lallemand et al., 2016). Phytoplankton biomass is a biophysical parameter commonly used to assess the eutrophic status of coastal water bodies. In particular, the photosynthetic pigment chlorophyll-a (chl-a) is an indicator of phytoplankton biomass. Therefore, it is crucial to provide information on the changes of the marine ecosystem and water biogeochemical parameters, such as turbidity and chl-a, during a volcanic eruption (Shi and Wang, 2011; Mantas et al., 2011). Previous studies during volcanic eruptions in the El Hierro Island (Canary Islands) evaluated both water quality parameters with

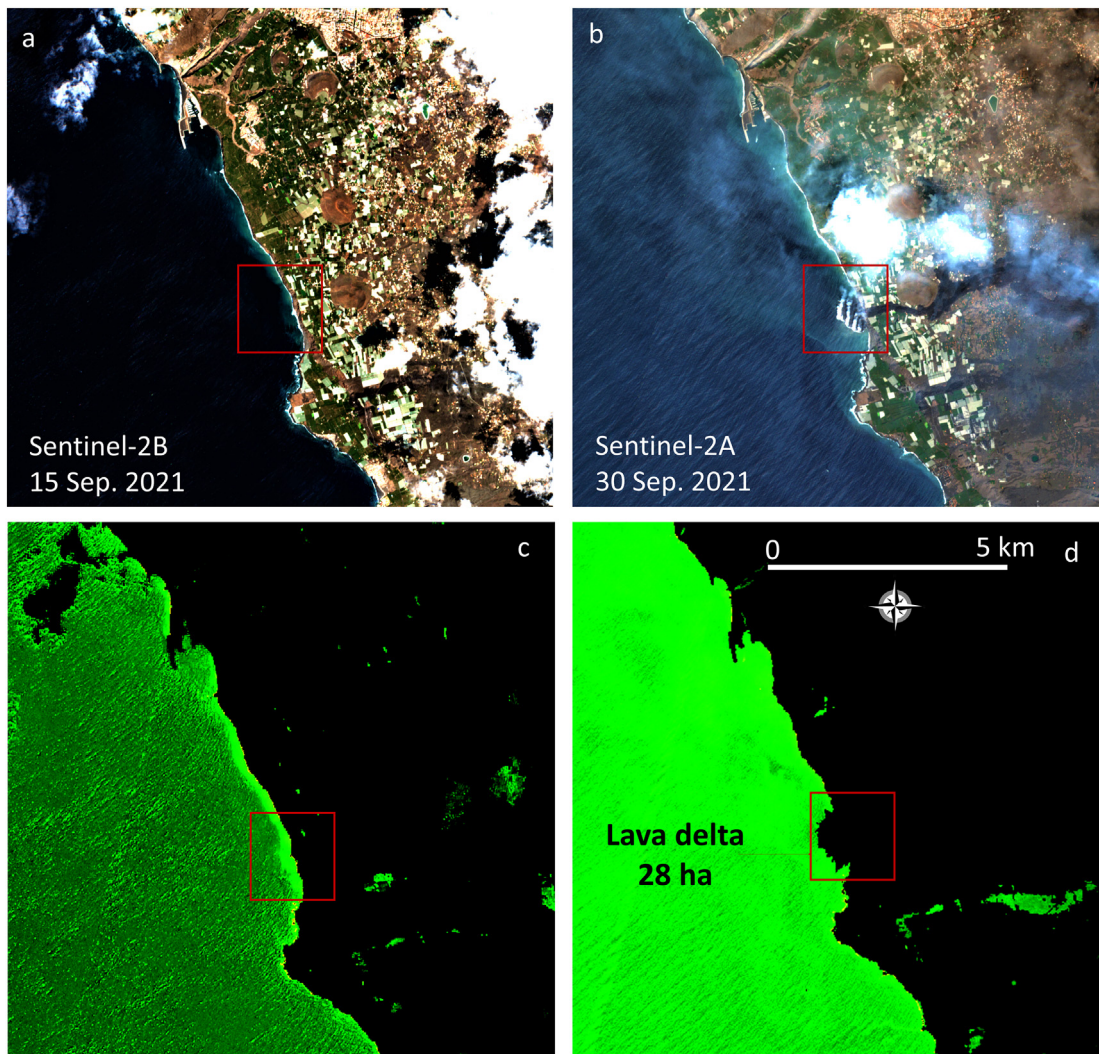


Fig. 3. a) Sentinel-2B RGB composited (Red-Green-Blue) pre-eruption scene acquired on 15 September 2021, b) Sentinel-2A RGB composited (Red-Green-Blue) post-eruption scene acquired on 30 September 2021; map of the coastline c) before (on 15 September 2021) and d) after (30 September 2021) the lava delta formation on the western section of La Palma.

moderate and high-resolution spatial satellite imagery as key variables of the ecological status of the coastal water masses (Fraile-Nuez et al., 2012; Coca et al., 2014; Eugenio et al., 2014). Water resources management could be addressed by using optical satellite data, which can help in quantifying the impact on the marine environment and understanding coastal processes, especially during and after natural hazards, in addition to support sustainable development in data-poor regions (Sheffield et al., 2018). Rafts and volcanic plumes discolor surrounding waters depending on their characteristics (lava flows, bubbles of lava, ashes, volcanic plumes and pumice) (Siebert and Simkin, 2013a, 2013b). The chemical composition of discolored seawater, which is one of the characteristics of volcanic activity, can be estimated from remote-sensing data after a robust atmospheric correction (Urai and Machida, 2005). Recent studies displayed the potential of atmospherically corrected surface reflectance from satellite to develop the equation between the color and chemical composition of discolored seawater around a submarine volcano (Sakuno, 2021). The relationship between the chemical composition of discolored seawater and volcanic activity has been already investigated (Nogami et al., 1993), evaluating the chemical composition conducted using remote sensing (Urai and Machida, 2005; Sakuno, 2021).

Remote sensing techniques can be a complementary, synoptic and powerful tool for coastal managers to improve current monitoring, as well as to provide insights during catastrophes, disasters or environmental crisis.

Although cloud cover over islands can be high, remote sensing is an accessible and useful tool for short- and long-term water quality studies. In this regard, high-resolution optical missions may enable novel coastal observations and water quality mapping that lead to new questions. Although ocean color sensors provide a unique synoptic view of surface water bi-optical conditions across scales not feasible with field-based monitoring techniques, applications in coastal biogeochemical monitoring is challenging. Recent research suggested that, in order to properly detail the status of coastal regions through satellite data, enhanced spatial resolution might be utilized over complex coastal water areas (Fraile-Nuez et al., 2012; Eugenio et al., 2014; Pahlevan et al., 2019; Aubriot et al., 2020; Caballero et al., 2020; Chen et al., 2020; Cao and Tzortziou, 2021). High-resolution satellite imagery was already used to document and map the various morphologic changes that occurred throughout the duration of volcanic eruptive periods (Achmad et al., 2019; Waythomas et al., 2020). Initially designed for terrestrial applications, the significantly improved spatial resolution and smaller footprint of both Sentinel-2 and Landsat-8 satellite missions offer an optimal opportunity to detect the dynamic spatial heterogeneity that characterizes terrestrial-aquatic environments and their interfaces at local, regional, and global scales (Page et al., 2019; Zhang et al., 2020).

Therefore, this study examined the main descriptors of the water quality during the volcanic eruption of La Palma using the high-resolution Sentinel-2 and Landsat-8 satellites in tandem. Pre-, syn-, and post-eruption water

quality maps were successively generated with the multi-sensor approach, allowing us to evaluate the evolution of the biogeochemical parameters in a region adjacent to the new lava delta. The key objectives of the present study were: (1) to implement a robust and consistent pre-processing framework (atmospheric and sunglint corrections) with the optical multi-sensor approach for both Sentinel-2 and Landsat-8 satellites in La Palma; (2) to characterize the fine-scale bio-optical features and temporal gradients of the water quality parameters of relevance, i.e. turbidity and chlorophyll-a concentration, during the study period; and (3) to assess and identify the main changes and critical areas using the retrieval products in the context of the latest volcanic disaster. The La Palma eruption provided a unique opportunity to quantify the catastrophic event's transitory impact on water quality as part of a time series study, which, to the best of our knowledge, was not monitored within CEMS Rapid Mapping (EMSR546). This exploratory research and the ability to rapidly process and visualize outcomes across the entire island has an increasing potential to generate new techniques and enhance the analysis of Earth Observation data for management, emergency and scientific research.

2. Methods

2.1. Satellite imagery

The Sentinel-2 twin satellites were used for monitoring the water quality due to their high spatial resolution (10–20–60 m) and open data access policy. The European Commission (EC) and the European Space Agency (ESA) developed the Sentinels constellation to meet the operational needs of the Copernicus programme. Sentinel-2 is a multispectral imaging mission, which supports Copernicus Land Monitoring studies, including the monitoring of soil and water cover, vegetation, as well as observation of coastal areas and inland waterways. The mission is based on a constellation of two operational identical satellites, Sentinel-2A and Sentinel-2B in the same orbit, phased at 180° to each other. Due to its high-revisit frequency and mission coverage, it provides for the generation of geoinformation at local, regional, and national scales. The multispectral instruments (MSI) on-board Sentinel-2A and Sentinel-2B satellites are operational with a global revisit frequency of five days at the Equator. The radiometric, spectral and spatial characteristics of the visible and near-infrared (NIR) bands used in this study are specified in the User Handbook (European Space Agency, 2015). Sentinel-2 scenes are geo-located within two pixels (20 m) which is within the stated quality requirements for absolute geolocation (European Space Agency, 2017). The scenes covering La Palma Island (zone 28 and tile RBS; acquisition time ~12:00 UTC) during four consecutive months (September–December 2021) were downloaded from the Copernicus Open Access Hub. These images corresponded to Level-1C (L1C) radiometrically and geometrically corrected top of atmosphere (TOA) products.

Moreover, we also used Landsat-8 imagery for detailed mapping at a 30 m spatial resolution. These observations are available from the National Aeronautics and Space Administration (NASA) and the Department of the Interior U.S. Geological Survey (USGS). Landsat-8 acquires imagery of the Earth's terrestrial and polar regions in the visible and NIR spectra with a 16-day revisit frequency, with enhanced signal-to-noise ratio and 12-bit radiometric resolution (Woodcock et al., 2008; Knight and Kvaran, 2014). Orthorectified and terrain corrected Level 1 images during September–December 2021 were downloaded from Earth Explorer (<https://earthexplorer.usgs.gov/>). The tiles corresponding to the region of interest were located in path 208 and row 40 (acquisition time ~11:45 UTC).

Only scenes with low cloud coverage (<40%) over the island were selected for further analysis (see Table 1 for acquisition dates of both Sentinel-2 and Landsat-8). From the total number of scenes during the study period, 23 and 8 for Sentinel-2 and Landsat-8, respectively, only 9 and 5 were further evaluated due to cloud and volcanic ash cover and sunglint contamination after processing.

Table 1

List of imagery used in this study corresponding to the Sentinel-2 and Landsat-8 satellites from September to December 2021. Mean surface seawater turbidity and chlorophyll-a concentration calculated for each cloud free scene within the region of interest (ROI, detailed in Fig. 5) in the western coast of La Palma Island.

Satellite	Month	Day	Observations	Turbidity (FNU)	Chlorophyll-a (mg/m ³)
Sentinel-2B	September	5	Intense sunglint	–	–
Landsat-8	September	10	Low sunglint	1.7	0.18
Sentinel-2B	September	15	Low sunglint	1.9	0.21
Sentinel-2A	September	20	Clouds	–	–
Sentinel-2B	September	25	Low sunglint	1.8	0.19
Landsat-8	September	26	Low sunglint	1.5	0.18
Sentinel-2A	September	30	Low sunglint	4.2	0.17
Sentinel-2B	October	5	Clouds/volcanic ash	–	–
Sentinel-2A	October	10	Clouds/volcanic ash	–	–
Landsat-8	October	12	Clouds/volcanic ash	–	–
Sentinel-2B	October	15	Low sunglint	10.2	0.39
Sentinel-2A	October	20	Clouds/volcanic ash	–	–
Sentinel-2B	October	25	Clouds/volcanic ash	–	–
Landsat-8	October	28	Low sunglint	9.7	0.25
Sentinel-2A	October	30	Clouds/volcanic ash	–	–
Sentinel-2B	November	4	Clouds/volcanic ash	–	–
Sentinel-2A	November	9	Clouds/volcanic ash	–	–
Landsat-8	November	13	Clouds/volcanic ash	–	–
Sentinel-2B	November	14	Low sunglint	2.9	0.21
Sentinel-2A	November	19	Clouds	2.8	0.17
Sentinel-2B	November	24	Clouds/volcanic ash	–	–
Sentinel-2A	November	29	Clouds	2.5	0.19
Landsat-8	November	29	Clouds/volcanic ash	–	–
Sentinel-2B	December	4	Clouds/volcanic ash	–	–
Sentinel-2A	December	9	Clouds/volcanic ash	–	–
Sentinel-2B	December	14	Low sunglint	2.4	0.18
Landsat-8	December	15	Low sunglint	2.8	0.17
Sentinel-2A	December	19	Clouds/volcanic ash	–	–
Sentinel-2B	December	24	Clouds/volcanic ash	–	–
Sentinel-2A	December	29	Low sunglint	3.4	0.24
Landsat-8	December	31	Low sunglint	2.2	0.25

2.2. Atmospheric correction and water quality mapping

The Level-1C images were atmospherically corrected to Level-2A (bottom of atmosphere, BOA) with the commonly used ACOLITE processor (version 20210114.0). ACOLITE uses an image-based approach that does not require in-situ atmospheric information. ACOLITE was specifically developed for marine, coastal, and inland waters by the Royal Belgian Institute of Natural Sciences (RBINS) and supports free processing of Landsat-8 and Sentinel-2 satellites (Vanhellemont and Ruddick, 2016). We selected a novel algorithm within the ACOLITE toolbox, the Dark Spectrum Fitting (DSF) atmospheric correction model (Vanhellemont and Ruddick, 2018; Vanhellemont, 2019). This recent algorithm was initially developed for water applications of meter-scale optical satellites but has already demonstrated its potential for application to both Landsat-8 and Sentinel-2 satellites due to their improved spectral coverage, notably including bands in the short wave infrared region (Vanhellemont, 2019). We also selected the optional image-based sunglint correction of the surface reflectance since during the study period sunglint contamination was observed at Level-1C. ACOLITE products correspond to remote sensing reflectance (R_{rs} , sr^{-1}) in all visible and NIR bands, resampled to 10 m pixel size for Sentinel-2 and 30 m for Landsat-8.

In order to evaluate the water quality parameters during the eruption crisis, we selected turbidity (FNU) and chlorophyll-a (mg/m^3) as standard products. The assessment of the good ecological status of the coastal waters in the context of the EU Water Framework Directive (WFD) includes both indicators, turbidity and chlorophyll-a. Final water quality products were at 10 m and 30 m spatial resolution for Sentinel-2 and Landsat-8, respectively. Data were flagged using the standard land and cloud masking as well as poor performance of the atmospheric correction. The process of downloading and processing each of these images was completed in ~4 h following image acquisition for each tile.

In this study, turbidity was estimated applying a semi-analytical algorithm by Nechad et al. (2009, 2010) using the remote sensing reflectance of the red band (R_{rs} 665 nm) of both Sentinel-2 and Landsat-8. This algorithm has already been used in several environments (Katlane et al., 2013; Caballero et al., 2019; Nazirova et al., 2021; Vanhellemont and Ruddick, 2021). These semi-analytical models are based on the inherent optical properties of the water and provide a more global application. The concentration of water chlorophyll-a was computed using the commonly used OC3 algorithm, a three banded maximum band ratio that uses fourth order polynomial function as a proxy of the chlorophyll-a bloom (Vanhellemont, 2019). The OC3 chl-a model was already used in the Canary Islands with the Moderate-Resolution Imaging Spectroradiometer (MODIS) onboard the AQUA satellite (Coca et al., 2014), in particular in El Hierro submarine volcano eruption during 2011 (Fraile-Nuez et al., 2012).

3. Results and discussion

3.1. Pre-processing scheme

During the study period from September to December 2021, a total of 23 Sentinel-2 and 8 Landsat-8 scenes were acquired and processed. When these products are combined as a constellation, the mean revisit time at this latitude is ~ 4 days. However, only 14 scenes ($\sim 45\%$ of the total scenes) were further evaluated under the lowest cloud and volcanic ash coverage to clarify the spatiotemporal variation of water quality (see Table 1 for details). Fig. 1d-f shows a Sentinel-2 RGB (Red-Green-Blue) composited image on 30 September, 10 and 15 October 2021 at 10 m spatial resolution after the volcanic eruption. Sentinel-2 satellites, although initially not designed

for coastal ocean applications, are key tools for detailed monitoring of heterogeneous environments, including inland water cover and coastal areas.

Robust atmospheric and sunglint correction approaches are required to thoroughly address the ecological status of the coastal waters adjacent to La Palma Island using remote sensing technologies (Vanhellemont and Ruddick, 2016; Vanhellemont and Ruddick, 2018; Vanhellemont, 2019; Vanhellemont and Ruddick, 2021). The sunglint (specular reflection of sunlight off the water) also affected the high-resolution imagery during the study period. In particular, at these latitudes, moderate sunglint contamination of both Landsat-8 and Sentinel-2 was encountered (see Table 1 for details). Fig. 4 indicates two scenes on 26 and 30 September 2021 for Landsat-8 and Sentinel-2, respectively, at top-of-atmosphere (TOA) Level 1, bottom-of-atmosphere (BOA) Level 2 after ACOLITE, and the remote sensing reflectance (R_{rs}) of the blue band (wavelength of 483–492 nm). ACOLITE performed properly for low to moderate sunglint conditions, retrieving information over these complex areas. The sunglint is visible at BOA level (Fig. 4a, d), whereas minimal residuals are visible at TOA level (Fig. 4b,e) and R_{rs} of the blue band (Fig. 4c,f). Similar outcomes have been obtained in other areas of the world, such as the Caribbean waters (Caballero and Stumpf, 2020) and North Atlantic waters (Caballero et al., 2020). Atmospheric correction over inland and coastal waters is one of the major remaining challenges in aquatic remote sensing, often hindering the quantitative retrieval of biogeochemical variables and analysis of their spatial and temporal variability within aquatic environments (Pahlevan et al., 2021). Several studies already suggested that ACOLITE offers precise information for aquatic system applications (Vanhellemont and Ruddick, 2016, 2018, 2021; Vanhellemont, 2019). Occasionally, residual sunglint suggested the need for improvements in the atmospheric correction procedure to empower the application community to extensively explore Landsat-8 and Sentinel-2 products. Recognizing

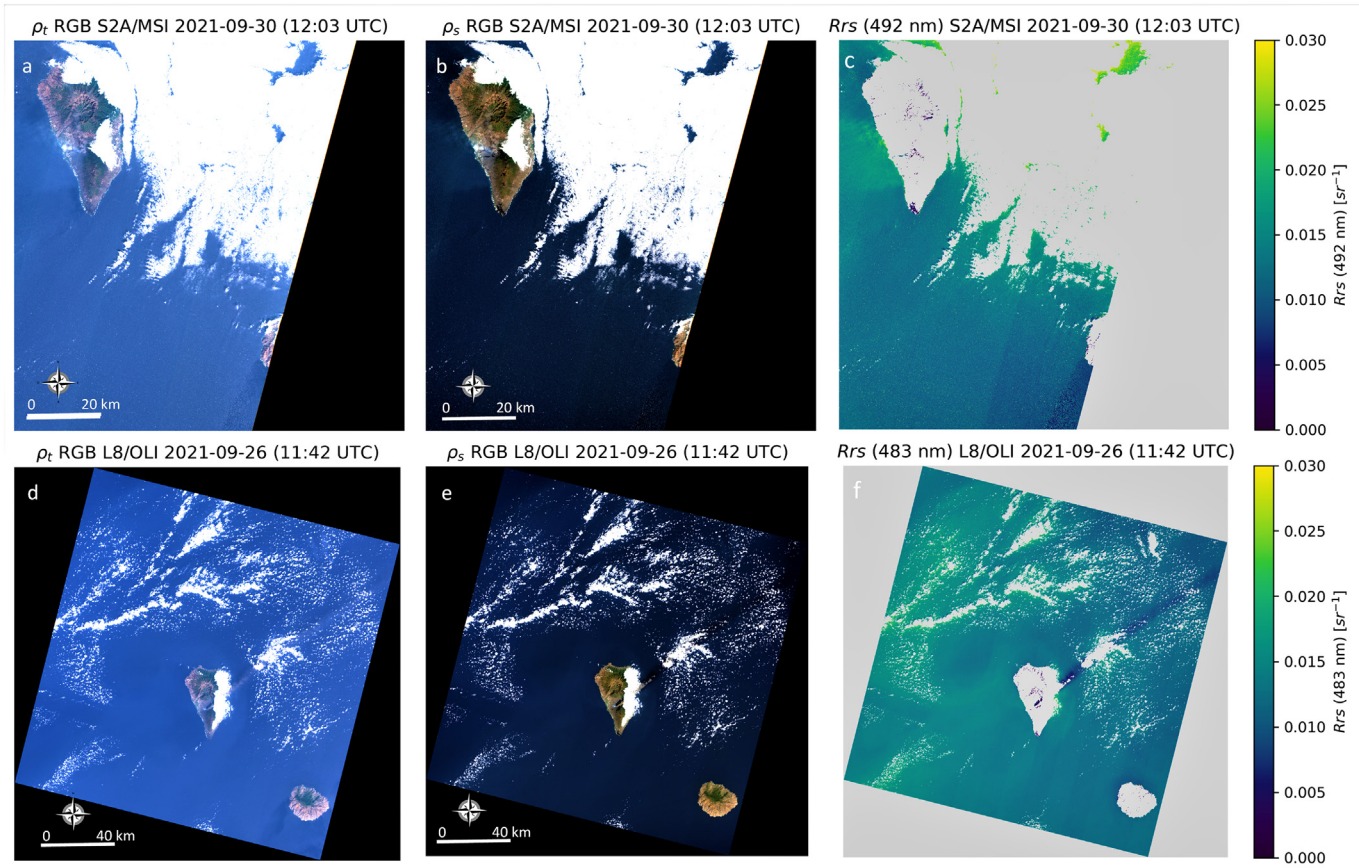


Fig. 4. RGB (Red-Green-Blue) composited image on 30 September 2021 of the Sentinel-2A satellite (10 m spatial resolution) at a) Top-Of-Atmosphere (TOA) Level, b) Bottom-Of-Atmosphere (BOA) Level after ACOLITE, and c) Remote sensing reflectance (R_{rs} , sr^{-1}) of the blue band (492 nm); RGB (Red-Green-Blue) composited image on 26 September 2021 of the Landsat-8 satellite (30 m spatial resolution) at d) Top-Of-Atmosphere (TOA) Level, e) Bottom-Of-Atmosphere (BOA) Level after ACOLITE, and f) Remote sensing reflectance (R_{rs} , sr^{-1}) of the blue band (483 nm).

the differences in spatial and spectral sampling under various atmospheric, sunglint and aquatic conditions to create a data record for coastal and inland water quality monitoring is a critical task (Pahlevan et al., 2019, 2021). This information is vital to ensure a precise near-real time monitoring with Sentinel-2 and Landsat-8 satellites working in tandem.

3.2. Water quality mapping

Fig. 5 displays the image-derived maps for surface seawater turbidity, with the imagery corresponding to the previous days before and after the onset of the volcanic eruption on 19 September 2021. The first observation derived from the collected data is that, as reported for surface turbidity, the western part of the island had markedly larger values and gradients, where recent lava flows entered the ocean. In general, the turbidity levels were very low (< 2 FNU) in the coastal area on 10, 15, 25 and 26 September 2021, before the formation of the lava delta. On 30 September, after the formation of the lava delta (**Fig. 3**), increased turbidity levels (~4 FNU) were observed in the western part of La Palma, and on 15 October, the turbidity was higher compared to previous days, with mean levels ~10 FNU and

reaching ~20 FNU in some regions. This volcanic plume appeared adjacent to the lava delta in the western part during mid-October. High turbidity levels with particle plumes persisted not only in the center of the western part, but also in the southwest. For the other regions, the turbidity of the water was similar to the pre-eruption condition. These plumes with discolored water of volcanic origin might have possible implications for algal communities since volcanoes inject large amounts of material with variable chemical composition into the oceans, thus being a potential source of trace metals and nutrients. The mean turbidity levels in the region of interest (ROI) close to the lava delta in the western section of the island (**Fig. 5**) are detailed in **Table 1**, highlighting an increase from pre- and syn-eruption situation as a result of eruptive ash and the lava delta altering ocean chemistry. The sudden break and the deterioration of the water quality on the western coast did not reach a stage of severe turbidity. After the formation of the lava delta in October, the ecosystem turbidity gradually recovered during November and December as can also be observed from the optical images in the decay of turbidity retrievals on the western side. However, the volcano continued to discharge from the land to the lava delta as indicated by CEMS Rapid Mapping (EMSR546). Remote sensing data also

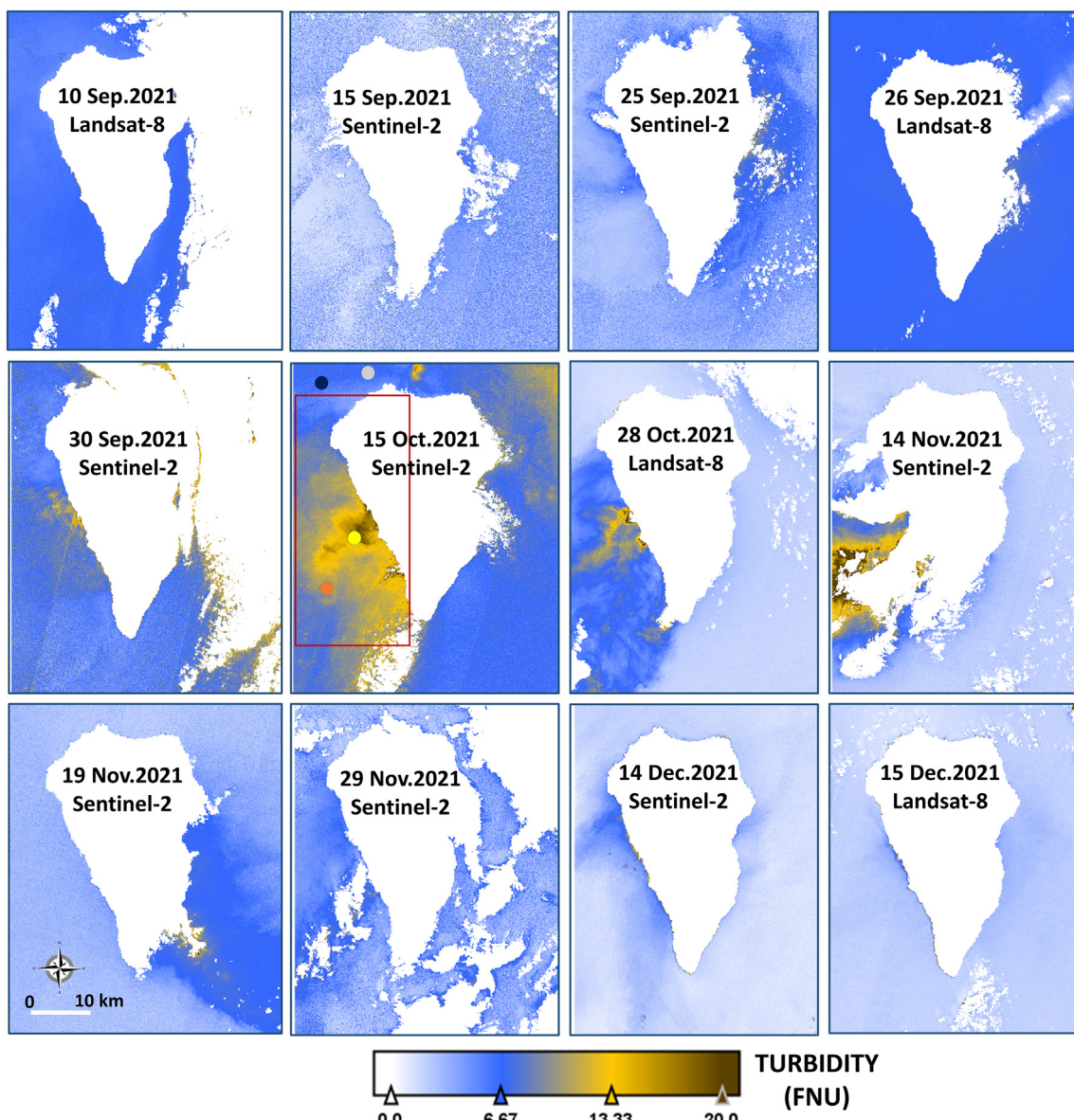


Fig. 5. Surface seawater turbidity (FNU) maps of the Sentinel-2 satellite (10 m spatial resolution) and Landsat-8 satellite (30 m spatial resolution) images over La Palma during the study period from September until December 2021. Only scenes with low cloud coverage were used. White color corresponds to masked data (land, clouds, volcanic ash).

played a fundamental role in analyzing the physical-chemical properties of the water around the submarine volcano of El Hierro Island during the 2011 eruption in the Canary Islands (Coca et al., 2014; Eugenio et al., 2014). Therefore, monitoring is key to assessing the persistence of turbid plumes due to the deposition of volcanic lava and ashes and whether they last longer than the main eruptive events.

Fig. 6 displays the surface seawater chl-a maps corresponding to the days before and after the onset of the volcanic eruption on 19 September 2021. The most common chl-a conditions during this period were usually $<0.3 \text{ mg/m}^3$, ranging from $0.1\text{--}0.39 \text{ mg/m}^3$ with oligotrophic waters observed around the island as well as close to the lava delta. As it can be observed in this temporal sequence, the chl-a concentration did not substantially increase in the western section after the lava delta formation; therefore, peaked plankton blooms occurring during the study period were not detected at mesoscale or sub-mesoscale. Consequently, there were no clear indicators of eutrophic conditions and algal blooms developed due to the fertilization of the volcanic eruption and formation of the lava strip. The typical low chl-a values were not swiftly altered towards eutrophic conditions during October, November or December 2021. However,

other studies suggested that a potential growth rate response following the phytoplankton bloom could occur after extreme weather events and natural hazards (Lebrero et al., 2019). Volcanic eruptions can trigger algal blooms where diffuse iron from volcanic ash interacts with water and fertilizes existing algae (Mantas et al., 2011; Lindenthal et al., 2013; Coca et al., 2014; Eugenio et al., 2014; Armon and Starosvetsky, 2015; Kim et al., 2020). Natural evidence for biological response to the seaward deposition of subduction zone volcanic particulate matter comes from satellite images and data of the bio-optical properties of seawater. Duggen et al. (2007) presented MODIS satellite data indicating seawater discoloration due to the seaward deposition of volcanic particulate matter and illustrating an increase of chl-a concentration caused by a phytoplankton bloom. A recent study indicated that during the Raikoke volcano eruption (Kuril Islands), visible satellite imagery showed expansion of the island's surface area and a possibly-linked algal bloom south of the island (McKee et al., 2021). The presence of the volcano-rich materials might restrict, stimulate or enhance the response by the phytoplankton community near the lava delta. During the La Palma eruption, the expected plume of discolored water did not trigger widespread blooms to occur, at least not observed during the cloudless days examined, so

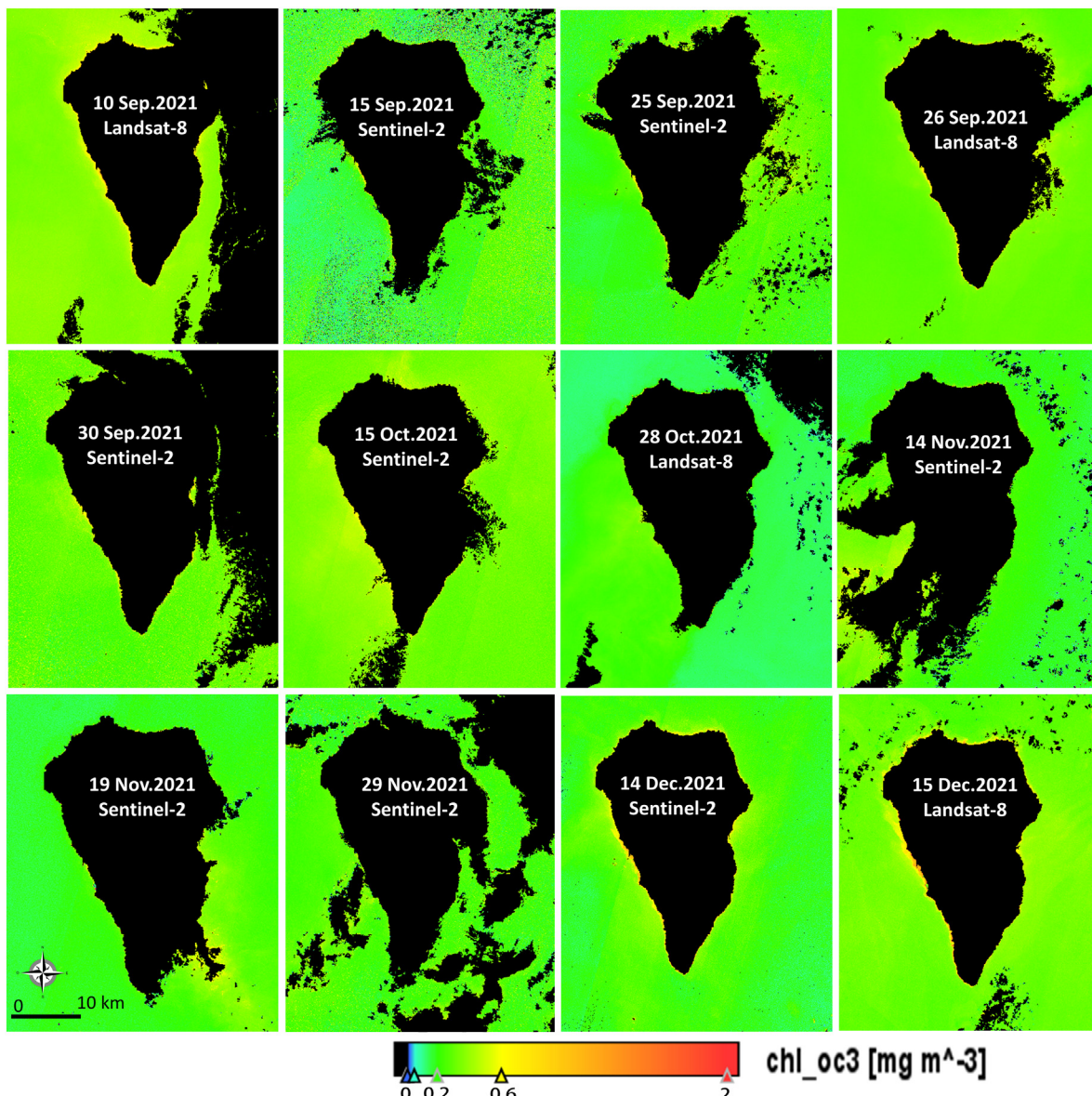


Fig. 6. Surface seawater chlorophyll-a concentration (Chl-a, mg/m^3) maps of the Sentinel-2 satellite (10 m spatial resolution) and Landsat-8 satellite (30 m spatial resolution) images over La Palma during the study period from September until December 2021. Only scenes with low cloud coverage were used. Black color corresponds to masked data (land, clouds, volcanic ash).

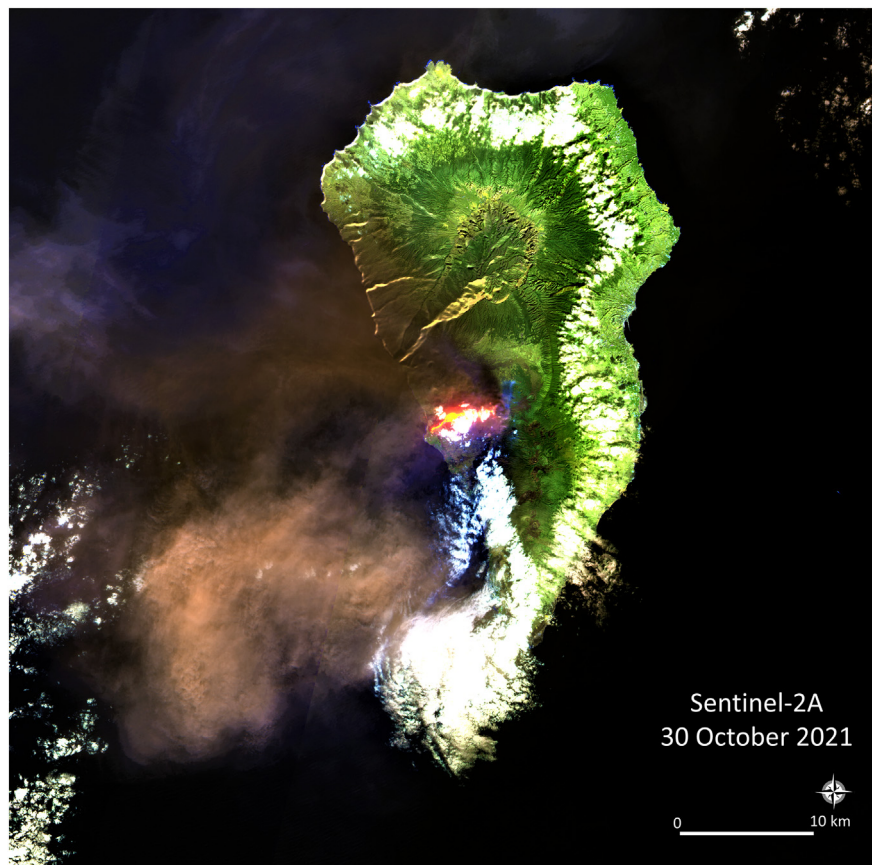


Fig. 7. Sentinel-2A RGB composited image acquired on 30 October 2021. The cloud and volcanic ash coverage remained very high over the west coast, so restricted information was retrieved from the optical imagery during October and December 2021.

the volcanic activity could be detrimental to biological communities. In the case of a time lag between the presence of the water plume and the phytoplankton blooms, this might be associated with the time necessary for the chemicals, such as iron input, to have significant impacts on the water (Mantas et al., 2011). In addition, the cloud and volcanic ash coverage remained very high on the west coast during the consecutive days of October–December 2021, as clearly observed in the RGB image acquired on 30 October 2021 (Fig. 7), so restricted information was retrieved over the surface seawater from the optical imagery.

Fig. 8 shows the spectral signature of the Sentinel-2 satellite on 15 October 2021 over four control points distributed along different areas (P1 and P3 in clear waters, P2 and P4 in the turbidity plume close to the lava delta; see Fig. 5 for location of the control points). The retrieved spectrum indicates remote sensing reflectance (R_{rs}) values for ocean and coastal waters in the vicinity of the lava delta. Interestingly, along the western coast, a change in the R_{rs} values was observed; far from the lava delta in the northern region, the radiometric signature resembled that of the typical ocean offshore waters, whereas within the plume, the R_{rs} changed progressively

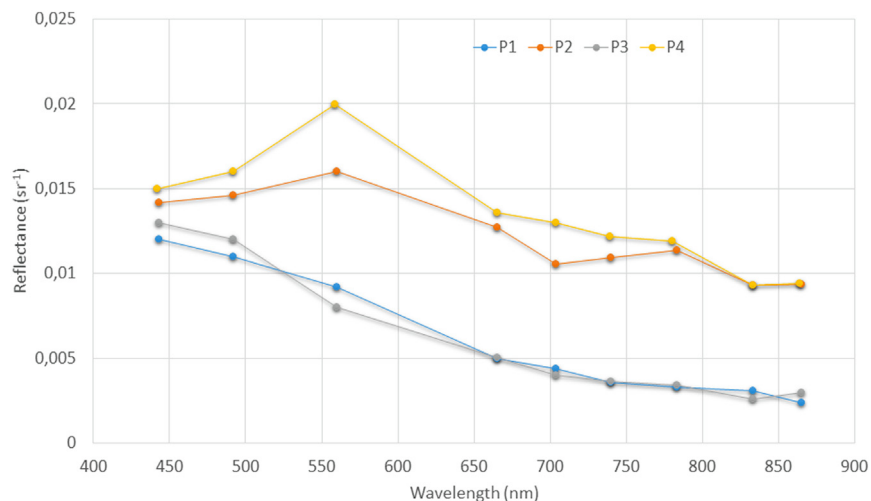


Fig. 8. Spectral signature of the Sentinel-2 satellite on 15 October 2021 over four control points distributed along different areas (P1 and P3 in offshore waters, P2 and P4 in the plume close to the lava delta). See Fig. 5 for location of the control points.

into a different spectrum with a distinctive drop in values for green, red, red-edge and near-infrared bands (560–850 nm). These preliminary results on discrimination of discolored seawaters by their reflectance patterns are similar to other studies (Urai and Machida, 2005; Mantas et al., 2011), further corroborating the remarkable value of these water quality products after the consistent atmospheric and sunglint correction of the ACOLITE processor. Shi and Wang (2011) also provided reflectance spectra for an ash-laden water after a volcanic eruption, indicating some unique optical features, similar to our results, and different from those of river plume waters or other productive waters.

On 25 December 2021, the local government declared the eruption to be officially over after three months, being the longest eruption recorded in the history of the island, and the most destructive in the last century in Europe (IGN, 2021). The satellite-measured water turbidity after one-week post-eruption on 29 and 31 December 2021 (Fig. 9) indicated that the environmental parameters returned to the pre-eruption condition and provided a clear picture of the water optical properties. The ash-laden

turbid waters near the eruption site disappeared. This suggests that at that time the coastal ocean environment nearly restored back to pre-eruption conditions. Fig. 10 displays the Sentinel-2 RGB composited scene on 29 December 2021, a post-eruption image, showing the lava delta in the north with a final area of 5 ha and the lava delta in the south with a final extension of 44 ha. These data can be used as an effective and efficient tool to synoptically monitor and assess the environmental changes.

3.3. Multi-sensor approach

Costly and time-consuming in situ measurements are frequently carried out to assess water quality over coastal areas during and after extreme weather events, hazards or catastrophes. Nevertheless, these approaches pose a risk for the technical personnel during the emergency and they may not address the complexity of the spatial and temporal variability. We proposed both Sentinel-2 and Landsat-8 missions in tandem to advance water control of La Palma during the 2021 volcanic eruption. The Sentinel-

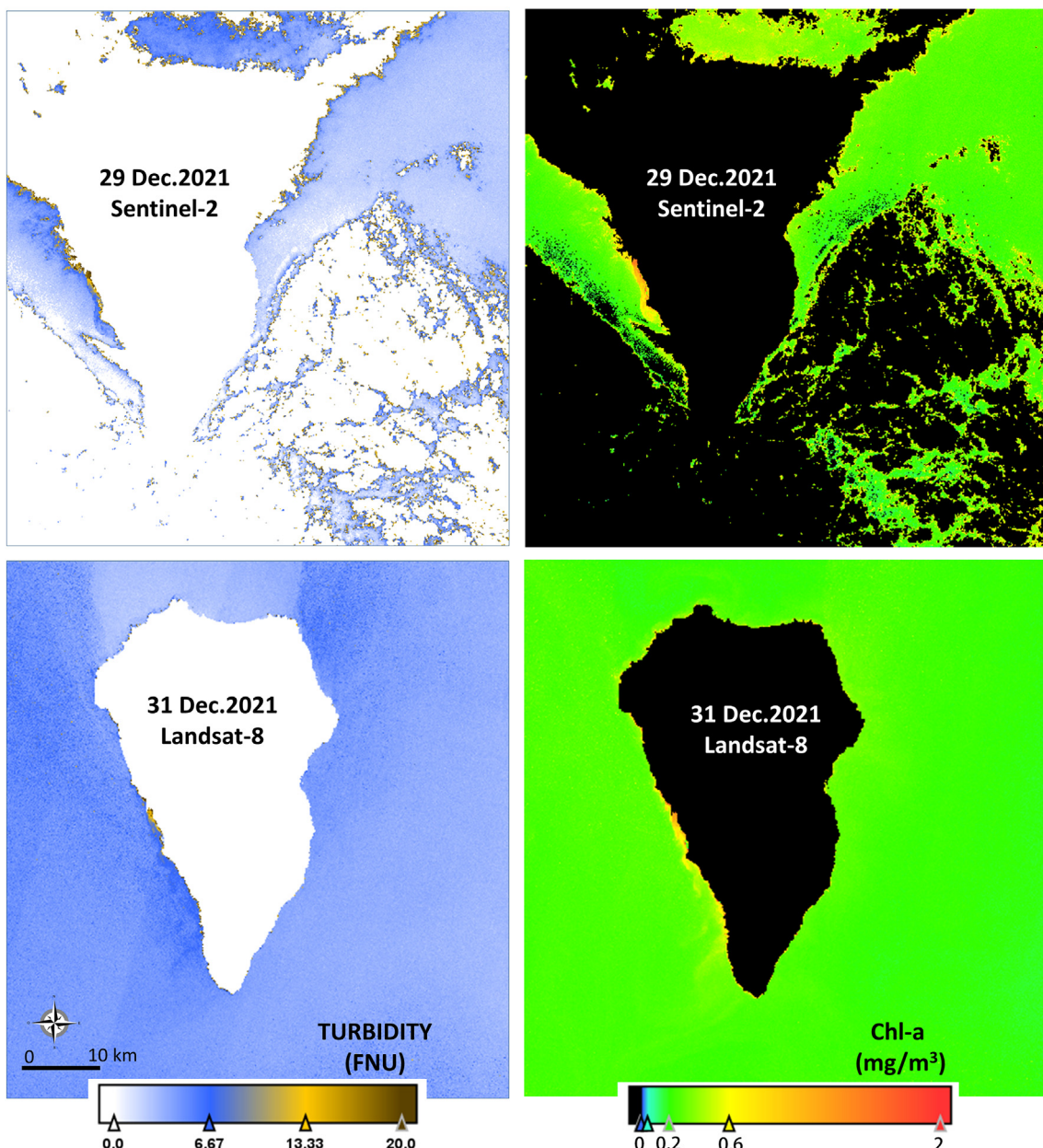


Fig. 9. Surface seawater turbidity (FNU) and chlorophyll-a concentration (Chl-a , mg/m^3) maps of the Sentinel-2 satellite (10 m spatial resolution) on 29 December 2021 and Landsat-8 satellite (30 m spatial resolution) on 31 December 2021 images over La Palma after the end of the volcanic eruption (25 December 2021).

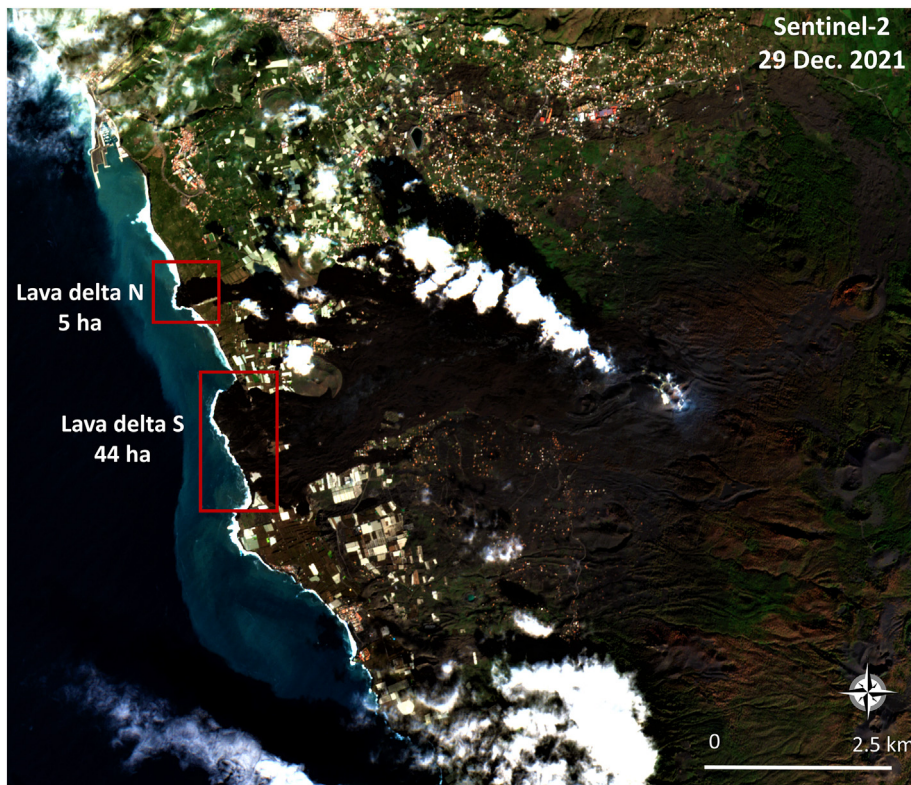


Fig. 10. Sentinel-2 post-eruption image of La Palma Island on 29 December 2021 showing the lava delta in the north with a final area of 5 ha and the lava delta in the south with a final extension of 44 ha.

2 and Landsat-8 constellations monitored and provided extensive and synoptic information of what was happening on La Palma, not only in land but also in the coastal waters adjacent to the island, as this study demonstrates. The variations of water quality that occurred before and after the sea was hit by the incandescent lava were determined in an adjacent perimeter, with anomalies registered in the marine conditions, both coastal and offshore waters, can profoundly reshape biogeochemical and ecological processes during one or two years at levels not previously observed in nature (Lebrero et al., 2019). The merged satellite data series revealed the complex nearshore features and fine-scale biogeochemical gradients across this dynamic coastal interface. The turbid plume observed on the western side was particularly challenging because its frequent small dimension prohibited the use of traditional ocean color remote sensing at low spatial resolution. Therefore, it is worth noting that finer resolution is required to properly address this spatio-temporal variability at typical scales of tens or hundreds of meters. Recent research suggested that, in order to comprehensively characterize the ecological status of complex coastal areas and land water inputs through satellite data, enhanced spatial resolution should be utilized by means of Landsat-8 and/or Sentinel-2 (Pahlevan et al., 2019; Caballero et al., 2020; Chen et al., 2020; Rodríguez-Benito et al., 2020).

High-resolution satellite imagery from Ikonos was also used to investigate the effects of flows from mud volcano eruptions from two aspects, the flood problem due to the sedimentation and the water quality problem in the river and estuary (Kure et al., 2014). Malawani et al. (2021) made a review of local and global impacts of volcanic eruptions and disaster management practices, highlighting that the impacts of volcanic eruptions on water bodies can have significant implications. However, hazards and management related to volcanic water quality, in particular for lakes, are poorly developed (Gunkel et al., 2008). Lallemand et al. (2016) evaluated the impact of the 2011 Puyehue-Cordon Caulle volcanic eruption (Chile), indicating that substantial environmental changes were observed after the eruption in association with the large amount of ash fallout. In that study, environment characterization was obtained through in situ observation and pre- and post-eruption visual assessment of publicly available Google

Earth satellite imagery, being turbidity the water quality variable that reflected the most changes throughout time. Waythomas et al. (2020) used high-resolution satellite imagery to allow documenting and mapping of the various morphologic changes that occurred on the subaerial part of Bogoslof Island during the volcanic eruptive period. Achmad et al. (2019) evaluated the geomorphological transition for affecting the coastal environment due to a volcanic eruption by means of high-resolution satellite imagery. Our multi-sensor approach might advance previous studies that aimed to characterize water quality over coastal and inland water masses during extreme weather events or catastrophes using coarser spatial resolution imagery (Mantas et al., 2011; Coca et al., 2014; Eugenio et al., 2014; Plank et al., 2020; McKee et al., 2021), as the complex variability of the coastal environment has been revealed in all the synoptic satellite-derived maps of the entire island presented.

Even though satellite products were not validated with local in situ data to address their quality and uncertainties, the turbidity and chl-a products used were proxies of the biogeochemical properties in the coastal waters of La Palma. We used the traditional OC3 model to quantify chl-a concentration and a commonly used semi-analytical model for the estimation of turbidity (Nechad et al., 2009, 2010; Vanhellemont, 2019). The latter has already been validated in several environments worldwide (Katlane et al., 2013; Caballero et al., 2018; Nazirova et al., 2021; Vanhellemont and Ruddick, 2021). These approaches are emerging as a valid and consistent methodologies in the study of turbidity and total suspended matter, which contribute to a more global application (Nechad et al., 2009, 2010; Wang et al., 2012). In addition, the OC3 chl-a model was already utilized in the Canary Islands, particularly in El Hierro submarine volcano eruption, providing accurate findings (Fraile-Nuez et al., 2012).

In conditions of high presence of clouds and volcanic ash coverage during volcanic eruption events, the amount of available and workable optical satellite data can be significantly reduced. In this sense, using a geostationary ocean color sensor, such as the Geostationary Ocean Color Imager (GOCI), should improve near-real-time water monitoring during volcanic events or hazards. The primary advantage of GOCI over other satellite

imagers is that it can obtain data every hour during the daytime, allowing coastal ocean monitoring effectively in quasi-real time. Several studies demonstrated the potential of GOCE for turbidity monitoring over coastal waters (Choi et al., 2012; Hu et al., 2016). In addition, other geostationary instruments, such as the Geostationary Korea Multi-Purpose Satellite (GK-2A), enhanced a developing method of volcanic ash detection (Lee and Lee, 2015). With three-to-four-day revisit time enabled by merged Landsat-8 and Sentinel-2 imagery, the coastal science and end-user community would benefit from high-quality and consistent products for synoptic operational purposes in the context of the EU Water Framework Directive (Cao and Tzortziou, 2021). However, it is clear that the presence of clouds and volcanic ash coverage are huge constraints to the use of optical (multispectral) data during volcanic eruptions events, as highlighted in this study. Nonetheless, the merged time-series products may contribute to most frequent observations at both short- and medium-term and enhanced monitoring of the subsequent water quality deterioration (Sheffield et al., 2018). This information offered an excellent opportunity to characterize the emplacement of the new lava delta and its impact on the marine environment in La Palma.

4. Concluding remarks

The September–December 2021 La Palma eruption was a complex event effectively monitored using remotely sensed data from a variety of sensors by the Copernicus Emergency Management Service (CEMS) Rapid Mapping. Sentinel-2 and Landsat-8 missions proved essential in tracking the development of the new lava delta and in measuring related eruption water quality impacts, such as turbidity or chl-a concentration, which were not regularly monitored by the CEMS Rapid Mapping. The possibility to collect detailed water quality maps before, during, and after the volcano eruption is fundamentally important for documenting the distribution and characteristics of the biogeochemical conditions adjacent to the new lava delta. An area close to the new lava-delta was observed where the physical-chemical properties of the water column, in particular turbidity, were significantly affected. Conversely, there was no pronounced chl-a change observed during and after the volcanic eruption in the region near the study site. High-resolution satellite technologies can play an essential role in the investigation of remote and past volcanic events in islands, which would have remained unnoticed otherwise. These favorable tools can be used in addition to routine on-site sampling methods to successfully mitigate the negative effects on the coastal waters after these catastrophic events in a very short time, facilitating prevention and security tasks and allowing access to risky areas during the emergency. With Sentinel-2A, Sentinel-2B, and Landsat-8 now operating, Landsat-9 already in orbit, new missions launching soon (e.g., Sentinel-2C and Sentinel-2D), and regularly advancing atmospheric correction techniques, the record of available high-resolution information is bound to be promptly expanded to offer an even more representative water quality characterization in the dynamic coastal environments. While scientists are developing enhanced satellite atmospheric and bio-optical algorithms, it is now the perfect time to consider, exploit and maximize this virtual constellation to provide timely assistance in coastal and inland water environments, in particular during environmental crisis and catastrophes, such as the 2021 volcanic eruption in La Palma.

CRediT authorship contribution statement

I. Caballero conceived and designed the research, collected the satellite data, processed the imagery, conducted the analysis and prepared figures. A. Román, A. Tovar-Sánchez, and G. Navarro collected and processed the unmanned aerial vehicle (UAV) data. I. Caballero led the writing of the manuscript with revision from A. Román, A. Tovar-Sánchez, and G. Navarro.

Declaration of competing interest

The authors declare that they have no known competing financial interests or personal relationships that could have appeared to influence the work reported in this paper.

Acknowledgments

This research was funded by grants RTI2018-098784-J-I00 (Sen2Coast Project) and IJC2019-039382-I (Juan de la Cierva-Incorporación) funded by MCIN/AEI/10.13039/501100011033 and by “ERDF A way of making Europe”. The research was also supported by the Regional Government (PY20-00244). A. Román is supported by the Spanish FPU Grant (Ref: FPU19/04557). Any opinions, findings, and conclusions or recommendations expressed in this material are those of the authors and do not necessarily reflect the views of the Spanish National Research Council (CSIC). The authors would like to thank the European Space Agency, the European Commission and the Copernicus programme for distributing Sentinel-2 imagery as well as the United States Geological Survey (USGS) and the National Aeronautics and Space Administration (NASA) for distributing Landsat-8 data. This work represents a contribution to CSIC Thematic Interdisciplinary Platforms PTI TELEDETECT and WATER:iOS. We also thank Martha B. Dunbar for her English language edits.

References

- Achmad, A.R., Syifa, M., Park, S.J., Lee, C.W., 2019. Geomorphological transition research for affecting the coastal environment due to the volcanic eruption of Anak Krakatau by satellite imagery. *J. Coast. Res.* 90 (SI), 214–220.
- Armon, R.H., Starovetsky, J., 2015. Algal bloom indicators. *Environmental Indicators. Springer, Netherlands, Dordrecht*, pp. 633–642.
- Aubriot, L., Zabaleta, B., Bordet, F., Sienra, D., Rissó, J., Achkar, M., Somma, A., 2020. Assessing the origin of a massive cyanobacterial bloom in the Río de la Plata (2019): towards an early warning system. *Water Res.* 181, 115944.
- Bacques, G., de Michele, M., Foumelis, M., Raucoules, D., Lemoine, A., Briole, P., 2020. Sentinel optical and SAR data highlights multi-segment faulting during the 2018 Palu-Sulawesi earthquake (M w 7.5). *Sci. Rep.* 10 (1), 1–11.
- Bosman, A., Casalbore, D., Romagnoli, C., Chiocci, F.L., 2014. Formation of an ‘a’ā lava delta: insights from time-lapse multibeam bathymetry and direct observations during the Stromboli 2007 eruption. *Bull. Volcanol.* 76 (7), 1–12.
- Caballero, I., Navarro, G., 2021. Monitoring cyanoHABs and water quality in Laguna Lake (Philippines) with Sentinel-2 satellites during the 2020 Pacific typhoon season. *Sci. Total Environ.* 788, 147700.
- Caballero, I., Stumpf, R.P., 2020. Atmospheric correction for satellite-derived bathymetry in the Caribbean waters: from a single image to multi-temporal approaches using Sentinel-2A/B. *Opt. Express* 28 (8), 11742–11766.
- Caballero, I., Ruiz, J., Navarro, G., 2019. Sentinel-2 satellites provide near-real time evaluation of catastrophic floods in the west Mediterranean. *Water* 11 (12), 2499.
- Caballero, I., Fernández, R., Escalante, O.M., Mamán, L., Navarro, G., 2020. New capabilities of Sentinel-2A/B satellites combined with in situ data for monitoring small harmful algal blooms in complex coastal waters. *Sci. Rep.* 10 (1), 1–14.
- Cao, F., Tzortziou, M., 2021. Capturing dissolved organic carbon dynamics with Landsat-8 and Sentinel-2 in tidally influenced wetland–estuarine systems. *Sci. Total Environ.* 777, 145910.
- Chen, J., Zhu, W., Tian, Y.Q., Yu, Q., 2020. Monitoring dissolved organic carbon by combining Landsat-8 and Sentinel-2 satellites: case study in Saginaw River estuary, Lake Huron. *Sci. Total Environ.* 718, 137374.
- Choi, J.K., Park, Y.J., Ahn, J.H., Lim, H.S., Eom, J., Ryu, J.H., 2012. GOCE, the world’s first geostationary ocean color observation satellite, for the monitoring of temporal variability in coastal water turbidity. *J.Geophys.Res.Oceans* 117 (C9).
- Coca, J., Ohde, T., Redondo, A., García-Weil, L., Santana-Casiano, M., González-Dávila, M., ... Ramos, A.G., 2014. Remote sensing of the El Hierro submarine volcanic eruption plume. *Int. J. Remote Sens.* 35 (17), 6573–6598.
- Corradino, C., Bilotta, G., Cappello, A., Fortuna, L., Del Negro, C., 2021. Combining radar and optical satellite imagery with machine learning to map lava flows at Mount Etna and Fogo Island. *Energies* 14 (1), 197.
- Di Traglia, F., Nolesini, T., Solaro, L., Ciampalini, A., Frodella, W., Steri, D., Casagli, N., 2018. Lava delta deformation as a proxy for submarine slope instability. *Earth Planet. Sci. Lett.* 488, 46–58.
- Duggen, S., Croot, P., Schacht, U., Hoffmann, L., 2007. Subduction zone volcanic ash can fertilize the surface ocean and stimulate phytoplankton growth: evidence from biogeochemical experiments and satellite data. *Geophys. Res. Lett.* 34 (1).
- Eugenio, F., Martin, J., Marcello, J., Fraile-Nuez, E., 2014. Environmental monitoring of El Hierro Island submarine volcano, by combining low and high resolution satellite imagery. *Int. J. Appl. Earth Obs. Geoinf.* 29, 53–66.
- European Space Agency, 2015. Sentinel-2 User Handbook, ESA Standard Document Paris, France. https://sentinel.esa.int/documents/247904/685211/Sentinel-2_User_Handbook.
- European Space Agency, 2017. Sentinel-2 MSI technical guide. <https://earth.esa.int/web/sentinel/technicalguides/sentinel-2-msi>.
- Fraile-Nuez, E., Marcello, J., Martin, J., 2012r. Monitoring El Hierro submarine volcano with low and high resolution satellite images. *Earth Resources And Environmental Remote Sensing/GIS Applications III. Vol. 8538. International Society for Optics and Photonics*, p. 853816.
- Gray, A., Krolkowski, M., Fretwell, P., Convey, P., Peck, L.S., Mendelova, M., Davey, M.P., 2020. Remote sensing reveals Antarctic green snow algae as important terrestrial carbon sink. *Nat. Commun.* 11 (1), 1–9.

- Gunkel, G., Beuker, C., Grupe, B., Viteri, F., 2008. Hazards of volcanic lakes: analysis of Lakes Quilotoa and Cuicocha, Ecuador. *Adv. Geosci.* 14, 29–33.
- Hu, Z., Pan, D., He, X., Bai, Y., 2016. Diurnal variability of turbidity fronts observed by geo-stationary satellite ocean color remote sensing. *Remote Sens.* 8 (2), 147.
- Instituto Geográfico Nacional, 2021. Informe mensual de vigilancia volcánica IGN. https://www.ign.es/web/resources/volcanologia/html/CA_noticias.html.
- Katlane, R., Nechad, B., Ruddick, K., Zargouni, F., 2013. Optical remote sensing of turbidity and total suspended matter in the Gulf of Gabes. *Arab. J. Geosci.* 6 (5), 1527–1535.
- Kim, K.B., Jung, M.K., Tsang, Y.F., Kwon, H.H., 2020. Stochastic modeling of chlorophyll-a for probabilistic assessment and monitoring of algae blooms in the Lower Nakdong River, South Korea. *J. Hazard. Mater.* 400, 123066.
- Knight, E.J., Kvaran, G., 2014. Landsat-8 operational land imager design, characterization and performance. *Remote Sens.* 6 (11), 10286–10305.
- Kure, S., Winarta, B., Takeda, Y., Udo, K., Umeda, M., Mano, A., Tanaka, H., 2014. Effects of mud flows from the LUSI mud volcano on the Porong River estuary, Indonesia. *J. Coast. Res.* 70 (10070), 568–573.
- Lallement, M., Macchi, P.J., Vigliano, P., Juarez, S., Rechencq, M., Baker, M., Crowl, T., 2016. Rising from the ashes: changes in salmonid fish assemblages after 30 months of the Puyehue-Cordon Caulle volcanic eruption. *Sci. Total Environ.* 541, 1041–1051.
- Lebrato, M., Wang, Y.V., Tseng, L.C., Achterberg, E.P., Chen, X.G., Molinero, J.C., Garbe-Schönberg, D., 2019. Earthquake and typhoon trigger unprecedented transient shifts in shallow hydrothermal vents biogeochemistry. *Sci. Rep.* 9 (1), 1–14.
- Lee, K.H., Lee, K.T., 2015. Volcanic ash retrieval using a new geostationary satellite. *Int. Arch. Photogramm. Remote Sens. Spat. Inform. Sci.* 40 (7), 67.
- Lindenthal, A., Langmann, B., Pätzsch, J., Lorkowski, I., Hort, M., 2013. The ocean response to volcanic iron fertilisation after the eruption of Kasatochi volcano: a regional-scale biogeochemical ocean model study. *Biogeosciences* 10, 3715–3729.
- Malawani, M.N., Lavigne, F., Gomez, C., Mutaqin, B.W., Hadimoko, D.S., 2021. Review of local and global impacts of volcanic eruptions and disaster management practices: the Indonesian example. *Geosciences* 11 (3), 109.
- Mantas, V.M., Pereira, A.J.S.C., Morais, P.V., 2011. Plumes of discolored water of volcanic origin and possible implications for algal communities. The case of the Home Reef eruption of 2006 (Tonga, Southwest Pacific Ocean). *Remote Sens. Environ.* 115 (6), 1341–1352.
- Martin, M.D., Barr, I., Edwards, B., Spagnolo, M., Vajedian, S., Symeonakis, E., 2021. Assessing the use of optical satellite images to detect volcanic impacts on glacier surface morphology. *Remote Sens.* 13 (17), 3453.
- McKee, K., Smith, C.M., Reath, K., Snee, E., Maher, S., Matoza, R.S., Perttu, A., 2021. Evaluating the state-of-the-art in remote volcanic eruption characterization part I: Raikoke volcano, Kuril Islands. *J. Volcanol. Geotherm. Res.* 419, 107354.
- Nazirova, K., Alferyeva, Y., Lavrova, O., Shur, Y., Soloviev, D., Bocharova, T., Strochkov, A., 2021. Comparison of in situ and remote-sensing methods to determine turbidity and concentration of suspended matter in the estuary zone of the Mzymta River, Black Sea. *Remote Sens.* 13 (1), 143.
- Nechad, B., Ruddick, K.G., Neukermans, G., 2009. SPIE Remote Sensing, Proceedings of the Remote Sensing of the Ocean, Sea Ice, Coastal Waters, and Large Water Regions 2009, Berlin, Germany, 31 August–3 September 2009; SPIE-International Society for Optics and Photonics: Bellingham, WA, USA. 7473. Calibration and validation of a generic multisensor algorithm for mapping of turbidity in coastal waters, p. 7473OH.
- Nechad, B., Ruddick, K.G., Park, Y., 2010. Calibration and validation of a generic multisensor algorithm for mapping of total suspended matter in turbid waters. *Remote Sens. Environ.* 114 (4), 854–866.
- Nogami, K., Yoshida, M., Ossaka, J., 1993. Chemical composition of discolored seawater around Satsuma-Iwojima, Kagoshima, Japan. *Bull. Volcanol. Soc. Jpn.* 38 (3), 71–77.
- Normandeau, A., Mackillop, K., Macquarrie, M., Richards, C., Bourgault, D., Campbell, D.C., Clarke, J.H., 2021. Submarine landslides triggered by iceberg collision with the seafloor. *Nat. Geosci.* 14 (8), 599–605.
- Page, B.P., Olmanson, L.G., Mishra, D.R., 2019. A harmonized image processing workflow using Sentinel-2/MSI and Landsat-8/OLI for mapping water clarity in optically variable lake systems. *Remote Sens. Environ.* 231, 111284.
- Pahlevan, N., Chittimalli, S.K., Balasubramanian, S.V., Vellucci, V., 2019. Sentinel-2/Landsat-8 product consistency and implications for monitoring aquatic systems. *Remote Sens. Environ.* 220, 19–29.
- Pahlevan, N., Mangin, A., Balasubramanian, S.V., Smith, B., Alikas, K., Arai, K., Warren, M., 2021. ACIX-Aqua: a global assessment of atmospheric correction methods for Landsat-8 and Sentinel-2 over lakes, rivers, and coastal waters. *Remote Sens. Environ.* 258, 112366.
- Plank, S., Walter, T.R., Martinis, S., Cesca, S., 2019. Growth and collapse of a littoral lava dome during the 2018/19 eruption of Kadovar Volcano, Papua New Guinea, analyzed by multi-sensor satellite imagery. *J. Volcanol. Geotherm. Res.* 388, 106704.
- Plank, S., Marchese, F., Genzano, N., Nolde, M., Martinis, S., 2020. The short life of the volcanic island New Late'iki (Tonga) analyzed by multi-sensor remote sensing data. *Sci. Rep.* 10 (1), 1–15.
- Rajendran, S., Sadooni, F.N., Al-Kuwari, H.A.S., Oleg, A., Govil, H., Nasir, S., Vethamony, P., 2021. Monitoring oil spill in Norilsk, Russia using satellite data. *Sci. Rep.* 11 (1), 1–20.
- Rodríguez-Benito, C.V., Navarro, G., Caballero, I., 2020. Using Copernicus Sentinel-2 and Sentinel-3 data to monitor harmful algal blooms in Southern Chile during the COVID-19 lockdown. *Mar. Pollut. Bull.* 161, 111722.
- Sakuno, Y., 2021. Trial of chemical composition estimation related to submarine volcano activity using discolored seawater color data obtained from GCOM-C SGII. A case study of Nishinoshima Island, Japan, in 2020. *Water* 13 (8), 1100.
- Sheffield, J., Wood, E.F., Pan, M., Beck, H., Coccia, G., Serrat-Capdevila, A., Verbist, K., 2018. Satellite remote sensing for water resources management: potential for supporting sustainable development in data-poor regions. *Water Resour. Res.* 54 (12), 9724–9758.
- Shi, W., Wang, M., 2011. Satellite observations of environmental changes from the Tonga volcano eruption in the southern tropical Pacific. *Int. J. Remote Sens.* 32 (20), 5785–5796.
- Siebert, L., Simkin, T., 2013. Volcanoes of the world: An illustrated catalog of Holocene volcanoes and their eruptions.
- Siebert, L., Simkin, T., 2013. Volcanoes of the world: an illustrated catalog of Holocene volcanoes and their eruptions.
- Tapete, D., Cigna, F., 2020. Poorly known 2018 floods in Bosra UNESCO site and Sergiopolis in Syria unveiled from space using Sentinel-1/2 and COSMO-SkyMed. *Sci. Rep.* 10 (1), 1–16.
- Urai, M., Machida, S., 2005. Discolored seawater detection using ASTER reflectance products: a case study of Satsuma-Iwojima, Japan. *Remote Sens. Environ.* 99 (1–2), 95–104.
- Vanhellemond, Q., 2019. Adaptation of the dark spectrum fitting atmospheric correction for aquatic applications of the Landsat and Sentinel-2 archives. *Remote Sens. Environ.* 225, 175–192.
- Vanhellemond, Q., Ruddick, K., 2016. ACOLITE processing for Sentinel-2 and Landsat-8: atmospheric correction and aquatic applications. *Living Planet Symposium Prague*.
- Vanhellemond, Q., Ruddick, K., 2018. Atmospheric correction of metre-scale optical satellite data for inland and coastal water applications. *Remote Sens. Environ.* 216, 586–597.
- Vanhellemond, Q., Ruddick, K., 2021. Atmospheric correction of Sentinel-3/OLCI data for mapping of suspended particulate matter and chlorophyll-a concentration in Belgian turbid coastal waters. *Remote Sens. Environ.* 256, 112284.
- Waythomas, C.F., Angeli, K., Wessels, R.L., 2020. Evolution of the submarine–subaerial edifice of Bogoslof volcano, Alaska, during its 2016–2017 eruption based on analysis of satellite imagery. *Bull. Volcanol.* 82 (2), 1–26.
- Woodcock, C.E., Allen, R., Anderson, M., Belward, A., Bindschadler, R., Cohen, W., Nemani, R., 2008. Free access to Landsat imagery. *Science* 320, 1011.
- Wulder, M.A., Coops, N.C., 2014. Satellites: make Earth observations open access. *Nat. News* 513 (7516), 30.
- Xu, W., Jónsson, S., 2014. The 2007–8 volcanic eruption on Jebel at Tair island (Red Sea) observed by satellite radar and optical images. *Bull. Volcanol.* 76 (2), 1–14.
- Zhang, X., Fichot, C.G., Baracco, C., Guo, R., Neugebauer, S., Bengtsson, Z., Fagherazzi, S., 2020. Determining the drivers of suspended sediment dynamics in tidal marsh-influenced estuaries using high-resolution ocean color remote sensing. *Remote Sens. Environ.* 240, 111682.
- Zhao, Z., Mitchell, N.C., Quartau, R., Ramalho, R.S., Rusu, L., 2020. Coastal erosion rates of lava deltas around oceanic islands. *Geomorphology* 370, 107410.